ՀԱՅԱՍՏԱՆԻ ԳԻՏՈՒԹՅՈՒՆՆԵՐԻ ԱԶԳԱՅԻՆ ԱԿԱԴԵՄԻԱՅԻ ՏԵՂԵԿԱԳԻՐ
ИЗВЕСТИЯ НАЦИОНАЛЬНОЙ АКАДЕМИИ НАУК АРМЕНИИ

Մեխանիկա 79, №1-2, 2026 Механика

УДК 539.3 DOI: 10.54503/0002-3051-2026.79.1-2-133

On Stiffened Composite Multilayer Cylindrical Shells

Alam M.F., Banafshi A., Moriel C., Hasanyan D.J., Hasanyan A.D.

Keywords: Cylindrical shell, Stability, Reinforced anisotropic shell.

М.Ф.Алам, А.Банафши, С.Мориел, Д.Дж.Асанян, А.Д.Асанян

Об усиленных многослойных цилиндрических оболочках из композитных материалов

Ключевые слова: цилиндрическая оболочка, устойчивость, усиленная анизотропная оболочка

Выведены уравнения для анализа колебаний/потери устойчивости цилиндрической композитной оболочки, состоящей из нескольких ортотропных слоев и усиленной эксцентрическими ребрами жесткости, под действием осевого сжатия, бокового давления и/или их комбинации, на основе теории Сандерса-Койтера. Нагрузки, вызывающие потерю устойчивости, получены с использованием теорий оболочек Сандерса-Койтера, Лява и Доннелла. Для дальнейшего представления теорий оболочек для определения нагрузки, вызывающей потерю устойчивости, рассмотрен следующий случай: перекрестно-слоистая конструкция из N, нечетно (симметрично) слоистых, ортотропных слоев. В некоторых случаях выведена аналитическая формула для нагрузки, вызывающей потерю устойчивости упрочненной изотропной цилиндрической оболочки, когда отношение основных жесткостей слоя равно 1. Из-за вариаций геометрических и физических параметров в теории, представление значимых общих результатов затруднено.

Три упомянутые выше теории сравниваются для нагрузок, вызывающих потерю устойчивости, в зависимости от расстояния между ребрами жесткости (кольцевыми ребрами жесткости). Показано, что упомянутые теории дают разные значения нагрузок, вызывающих потерю устойчивости. В некоторых случаях расхождение может достигать ~25%. Приводятся другие конкретные численные примеры для иллюстрации применения предложенной теории и выведенных аналитических формул для нагрузок, вызывающих потерю устойчивости. Кроме того, полученные здесь результаты сравниваются с аналогичными, ранее опубликованными, работами.

Ալամ Մ.Ֆ., Բանաֆշի Ա., Մորիել Ս., Հասանյան Դ.Ջ.,.Հասանյան Ա.Դ.

Ուժեղացված կոմպոզիտային բազմաշերտ գլանային թաղանթների մասին

Հիմնաբառեր՝ գլանային թաղանթ, կայունություն, ուժեղացված անիզոտրոպ թաղանթ

Սանդերս-Կոյտերի տեսության հիման վրա դուրս են բերված հավասարումներ առանցքային սեղման, կողային ճնշման կամ նրանց կոմբինացիայի ազդեցության տակ գտնվող մի քանի օրթոտրոպ շերտերից կազմված գլանային կոմպոզիտ թաղանթի տատանումների/կայունության կորստի ուսումնաիրման համար: Կայունության կորստի բերող բեռները ստացվել են սալերի Սանդերս-Կոյտերի, Լյավի և Դոնելի տեսությունների հիման վրա: Կայունության կորստի բերող բեռների որոշման սալերի տեսությունների հետագա ներկայացնելու նպատակով դիտարկվել է հետևյալ դեպքը՝ N կենտ (համաչափ) շերտավոր օրթոտրոպ շերտերից կազմված խաչաձև շերտավոր կոնստրուկցիա: Որոշ դեպքերում ուժեղացված իզոտրոպ գլանային թաղանթի, երբ շերտի հիմնական կոշտությունների հարաբերությունը հավասար է 1: Կայունության կորստի բերող բեռի հաշվարկման համար ստացվել է անալիտիկ բանաձև: Տեսության երկրաչափական և ֆիզիկական պարամետրերի փոփոխման լայն տիրույթի պատճառով նշանակալի ընդհանուր արդյունքների ներկայացումը դժվարություն է հարուցում:

Վերը նշված երեք տեսությունները համեմատվում են կայունության կորստի բերող բեռների համար՝ կախված կոշտության կողերի հեռավորությունից:Ցույց է տրված, որ նշված տեսությունները կայունության կորստի բերող բեռների տարբեր արժեքներ: Որոշ դեպքերում այն կարող է հասնել ~25%:

Բերված են այլ կոնկրետ թվային օրինակներ ցուցադրելու առաջարկված տեսության և արտածված անալիտիկ բանաձևերի կիրառության կայունության կորստի բերող բեռների համար: Ստացված արդյունքները համեմատվում են նախկինում ստացված աշխատանքների արդյունքների հետ:

Equations are derived for vibration/buckling analyses of a circular cylindrical shell with multiple orthotropic layers and eccentric stiffeners acting under axial compression, lateral pressure, and/or combinations based on Sanders-Koiter theory. Buckling loads are obtained using Sanders-Koiter, Love, and Donnell shell theories. To further demonstrate the shell theories for buckling load, the following case has been discussed: Cross-Ply with N odd (symmetric) laminated orthotropic layers. For certain cases the analytical buckling loads formula is derived for the stiffened isotropic cylindrical shell, when the ratio of the principal lamina stiffness is $F = E_2 / E_1 = 1$. Due to the variations in geometrical and physical parameters in theory, meaningful general results are complicated to present.

The three theories mentioned above are compared for buckling loads versus stiffeners (ring stiffened) spacing. It is shown that mentioned theories give different values for buckling loads. In some cases, disagreements can approach ~25%.

Accordingly, other specific numerical examples are given to illustrate application of the proposed theory and derived analytical formulas for the buckling loads. Also, the results derived herein are then compared to similar published work.

Keywords: Cylindrical shell, Stability, Reinforced anisotropic shell.

Nomenclature

$\mu_s = \dfrac{E_s A_s}{E_1 d_s h}\left(1-\nu_{12}\nu_{21}\right)$ - dimensionless stiffener rigidity

$\mu_r = \dfrac{E_r A_r}{E_1 d_r h}\left(1-\nu_{12}\nu_{21}\right)$ - dimensionless ring rigidity

$\eta_s = \dfrac{G_s A_s}{E_1 d_s h}\left(1-\nu_{12}\nu_{21}\right)\dfrac{J_s}{A_s L^2}$ - dimensionless torsional rigidity of stiffener

$\eta_r = \dfrac{G_r A_r}{E_1 d_r h}\left(1-\nu_{12}\nu_{21}\right)\dfrac{J_r}{A_r L^2}$ - dimensionless torsional rigidity of rings

$F = \dfrac{E_2}{E_1}$ - ratio of principal lamina stiffness

$R = \dfrac{1}{M+1} + \dfrac{8M\left(M-1\right)}{N^2 (M+1)^3}$ - denoted expression

$M = \dfrac{\sum_{k=odd} h_k}{\sum_{k=even} h_k}$ - called the cross-ply ratio

$G = \dfrac{G_{12}\left(1-\nu_{12}\nu_{21}\right)}{E_1}$ - non-dimensional shear modulus

$I_1 = \dfrac{I_s}{A_s L^2}$ - dimensionless moment of inertia for stiffeners

$I_2 = \dfrac{I_r}{A_r L^2}$ - dimensionless moment of inertia for rings

d_s - stiffener spacing

d_r - ring spacing

e_s - distance from stiffener centroid to shell reference surface, positive when stiffener is on outside

e_r - distance from rings centroid to shell reference surface, positive when rings are on outside;

h_k - thickness of k -th layer

E_1 and E_2 - Young's modulus of two perpendicular directions

ν_{12} and ν_{21} - Poisson's ratios

INTRODUCTION

It is well known that composite materials offer the potential for lighter weight and more efficient structures for various engineering applications. For instance, aerospace structures such as wings or fuselages are predominantly assemblies of shell structures. Pressure vessels are another common application where shell theory is applied in the design and subsequent fabrication of components. The analysis of composite shell structures has been of considerable interest to researchers due to the increasing use of composites in the design and construction of components in industry. The rise in use of composites in engineering applications can be directly attributed to the fact that composite designs produce lighter components than typical construction materials, with equal or greater strength and durability.

Shell theories developed for thin elastic shells are usually based on the Kirchhoff-Love hypothesis. Since ring stiffened composites have a low transverse shear modulus compared to isotropic materials, the Kirchhoff-Love hypothesis of non-deformable normal's is not strictly applicable for laminated, ring stiffened shell structures.

Leissa [16] provides an account and comparison of thirteen shell theories with proper assessment of both strain displacement relations and stress resultants.

In this paper, the theory accounting for rotation of shell elements around the mid-surface normal (Sanders-Koiter theory) is developed. In classic theories mentioned rotation is omitted for various reasons. If shells are stiffened local deformations can be created due to stiffeners. To capture local deformations (sometimes local buckling's due to stiffeners) without accountants of mid-surface normal can create significant disagreement between theoretical and realistic results.

The equations of motion and different aspects of stability and vibration of shells/plates have been discussed by many authors [1-34]. Recent bibliographies and review papers have also appeared in [14, 22, 32]. These theories involve the thinness assumption while still retaining the first order, shear-deformation approximation through the shell thickness. Donnell's theory neglects the contribution of the transverse shearing force intensity to the equilibrium of forces in the circumferential direction, while the Sanders-Koiter and Love shell theories include it. For this reason, the Donnell's shell theory is often referred to as Donnell quasi-shallow shell equations. Love and Donnell shell theories do not include the contribution of transverse and axial displacement in the twist terms. In view of these differences, it is important to establish the accuracy of these shell theories for composite circular cylindrical shell or panels, where the material could be anisotropic.

Stability studies of curved cylindrical shells with isotropic geometry under pressure, shear, and axial compression have been reported by many authors (see Leissa [16], Rafel [24], Rafel & Sandlin [25]). Further literature reveled that Gerard and Becker [9], as well as Jones [12-13], developed an exact solution for the buckling of a circular cylindrical shell with multiple orthotropic layers and eccentric stiffeners under axial compression. This theory enables the study of coupling between bending and extensional forces due to the presence of different layers in the shell and the presence of eccentric stiffeners. Critical design incentives were presented by James and Whitley [23] on the buckling strength of longitudinally stiffened curved plates. The buckling coefficient of stiffened curved plates was determined in terms of buckling coefficient of flat plate with the same edge restraint as

$$k = k_\infty + \frac{1}{k_\infty}\frac{12}{\pi^4}\left(\frac{d_s^2\sqrt{1-\nu^2}}{Rh}\right)^4,$$

where k_∞ is a buckling coefficient of flat plate; d_s is a stiffener spacing.

Governing equations or the statics and dynamics of reinforced composite shells are developed based on Vlasov's semi-membrane shell theory by Birman [4-5]. These equations have closed-form solutions illustrated for buckling and free vibration problems. The buckling solution converges to the known result for unstiffened isotropic shells.

Semites [30] discussed the general instability of eccentrically stiffened thin cylindrical panels under the action of three types of applied loads. The three loads are uniform axial compression, uniform hoop compression or lateral pressure, and uniform shear. The analysis is based on a small deflection theory for orthotropic shells which includes effects of stiffener eccentricity; stiffener spacing is assumed to be sufficiently small (smeared technique), the stiffener geometry is taken to be uniform, and the skin-stiffener connection is assumed to be monolithic. Effects of stiffener eccentricity, panel aspect ratio, and the curvature parameter is shown in graphical form.

The theoretical buckling strength of long curved plates in compression was investigated by Baruch and Singer [1]. The plates considered were supported against lateral deflection along their unloaded edges and were elastically restrained against rotation along those edges; hence, the plates considered may be reasonably representative of plates found in actual structures. They suggested an equation for stiffened curved plates from computing the buckling strength of a corresponding stiffened flat plate using a method such as the method of moment distribution.

Design information is presented on the buckling strength of longitudinally stiffened curved plates (see Jaunky et al [11]). Design charts for determining the buckling strength of flat plates stiffened longitudinally along the Z-section stringers were given for the plate support and similarly stiffener to the curved plate.

McElman et al [18-19] extended the work to include the effect of stiffeners on vibration and flutter. Correlation between theory and experiment was reported for static buckling loads by Card and Jones [6].

Yi-Wei et al [34] presented axial buckling loads for a circular cylindrical shell with a laminate, using a special stacking sequence. This showed that differences exist in buckling loads between results obtained using Sanders' equations and Donnell's equations, for some values of the fiber winding angle. These buckling loads were not compared to results from an analysis which is independent of any shell theory.

A linear analysis method is presented for the elastic stability of structures with uniform cross section that may be idealized as an assembly of laminated plate-strips, flat and curved, and beams (see Viswanathan and Tamakun [33]). Each plate-strip and beam cover the entire length of the structure and is simply supported on the edges normal to the longitudinal axis. Arbitrary boundary conditions may be specified on any external longitudinal side of plate-strips. The structure or selected plate-strips may be loaded in any desired combination of in-plane biaxial loads. The analysis simultaneously considers all modes of instability and is applicable for the buckling of laminated composite structures. Some numerical results are presented to indicate possible applications.

The primary objective of the present paper is to assess the accuracy of Sanders-Koiter, Love, and Donnell shell theories for buckling analysis using an analytical approach. These shell theories are commonly used due to their simplicity. Buckling loads for laminated and isotropic circular cylindrical curved panels are obtained for different geometrical parameters.

GENERAL DIFFERENTIAL EQUATIONS OF STABILITY OF STIFFENED CYLINDRICAL SHELLS: SANDERS-KOITER APPROACH

In this paragraph, the stability equations of cylindrical shells based on Sanders-Koiter theory is introduced. Using standard procedures, kinematics expressions shown in previous paragraph and equilibrium equations for multilayer composites, the Sanders-Koiter type stability differential equations for circular cylindrical shells can be derived at the following form

$$L_{ij}\left(U_j\right) - 2\rho h \frac{\partial^2 U_j}{\partial t^2} = G_{ij}\left(U_j\right) \tag{1}$$

where $L_{ij}\left(*\right)$ are operators introduced below

$$L_{11}\left(*\right) = A_{11}\frac{\partial^2}{\partial x^2} + \left(2A_{16} - B_{16}\frac{c_2}{R}\right)\frac{\partial^2}{\partial x \partial y} + \left(A_{66} - B_{66}\frac{c_2}{R} + D_{66}\frac{c_2}{4R^2}\right)\frac{\partial^2}{\partial y^2} \tag{2a}$$

$$L_{12}\left(*\right) = \left(A_{16} + \frac{3c_2}{2R}B_{16}\right)\frac{\partial^2}{\partial x^2} + \left[A_{12} + A_{66} + \frac{c_2}{R}\left(B_{12} + B_{66}\right) - \frac{c_2}{4R^2}D_{66}\right]\frac{\partial^2}{\partial x \partial y}$$
$$+\left(A_{26} + B_{26}\frac{c_2}{2R} - D_{66}\frac{c_2}{2R^2}\right)\frac{\partial^2}{\partial y^2} \tag{2b}$$

$$L_{13}(*) = \frac{A_{12}}{R}\frac{\partial}{\partial x} + \frac{1}{R}\left(A_{26} - B_{26}\frac{c_2}{R}\right)\frac{\partial}{\partial y} - B_{11}\frac{\partial^3}{\partial x^3} - \left[B_{12} + 2B_{66} - \frac{c_2}{R}D_{66}\right]\frac{\partial^2}{\partial x \partial y^2}$$

$$+\left(D_{16}\frac{c_2}{2R} - 3B_{16}\right)\frac{\partial^3}{\partial x^2 \partial y} + \left(D_{26}\frac{c_2}{2R} - B_{26}\right)\frac{\partial^3}{\partial y^3} \tag{2c}$$

$$L_{22}(*) = \left(A_{66} + \frac{3c_2}{R}B_{66} + \frac{9c_2}{4R^2}D_{66}\right)\frac{\partial^2}{\partial x^2} + \left[2A_{26} + \frac{9c_2}{2R}B_{26} + \frac{3c_2}{R^2}D_{26}\right]\frac{\partial^2}{\partial x \partial y}$$

$$+\left(A_{22} + 2B_{22}\frac{c_2}{R} + D_{22}\frac{c_2}{R^2}\right)\frac{\partial^2}{\partial y^2} \tag{2d}$$

$$L_{23}(*) = \frac{1}{R}\left(A_{26} + 3B_{26}\frac{c_2}{2R}\right)\frac{\partial}{\partial x} + \frac{1}{R}\left(A_{22} + B_{22}\frac{c_2}{R}\right)\frac{\partial}{\partial y}.$$

$$-\left(B_{16} + \frac{3c_2}{2R}D_{16}\right)\frac{\partial^3}{\partial x^3} - \left(3B_{26} + 7D_{26}\frac{c_2}{2R}\right)\frac{\partial^3}{\partial x \partial y^2}$$

$$-\left[B_{12} + 2B_{66} + \frac{c_2}{R}\left(D_{12} + 3D_{66}\right)\right]\frac{\partial^3}{\partial x^2 \partial y} - \left(B_{26} + \frac{c_2}{R}D_{26}\right)\frac{\partial^3}{\partial y^3} \tag{2e}$$

$$L_{33}(*) = D_{11}\frac{\partial^4}{\partial x^4} + 4D_{16}\frac{\partial^4}{\partial x^3 \partial y} + 4D_{26}\frac{\partial^4}{\partial y^3 \partial x} + D_{22}\frac{\partial^4}{\partial y^4} + 2\left(D_{12} + 2D_{66}\right)\frac{\partial^4}{\partial x^2 \partial y^2}$$

$$-2\frac{B_{12}}{R}\frac{\partial^2}{\partial x^2} - 2\frac{B_{22}}{R}\frac{\partial^2}{\partial y^2} - 4\frac{B_{26}}{R}\frac{\partial^2}{\partial x \partial y} + \frac{A_{22}}{R^2} \tag{2f}$$

$$L_{13} = L_{31}, \qquad L_{23} = L_{32} \tag{2g}$$

Force operators $G_{ij}(\bullet)$ have the following form

$$G_{11}(\bullet) = -\frac{c_1 c_2}{4}\frac{\partial}{\partial y}\left[\left(N_{xx}^0 + N_{yy}^0\right)\frac{\partial(\bullet)}{\partial y}\right], \quad G_{12}(\bullet) = \frac{c_1 c_2}{4}\frac{\partial}{\partial y}\left[\left(N_{xx}^0 + N_{yy}^0\right)\frac{\partial(\bullet)}{\partial x}\right],$$

$$G_{21}(\bullet) = \frac{c_1 c_2}{4}\frac{\partial}{\partial x}\left[\left(N_{xx}^0 + N_{yy}^0\right)\frac{\partial(\bullet)}{\partial y}\right],$$

$$G_{22}(\bullet) = \frac{c_2}{R^2}N_{yy}^0(\bullet) - \frac{c_1 c_2}{4}\frac{\partial}{\partial x}\left[\left(N_{xx}^0 + N_{yy}^0\right)\frac{\partial(\bullet)}{\partial x}\right],$$

$$G_{23}\left(\bullet\right)=-\frac{c_2}{R}\frac{\partial}{\partial y}\left[N_{xx}^0\frac{\partial\left(\bullet\right)}{\partial x}+N_{yy}^0\frac{\partial\left(\bullet\right)}{\partial y}\right],$$

$$G_{32}\left(\bullet\right)=-\frac{c_2}{R}\frac{\partial}{\partial x}\left(N_{xy}^0\left(\bullet\right)\right)-\frac{c_2}{R}\frac{\partial}{\partial y}\left(N_{yy}^0\left(\bullet\right)\right),$$

$$G_{33}\left(\bullet\right)=\frac{\partial}{\partial x}\left(N_{xx}^0\frac{\partial\left(\bullet\right)}{\partial x}+N_{xy}^0\frac{\partial\left(\bullet\right)}{\partial y}\right)+\frac{\partial}{\partial y}\left(N_{xy}^0\frac{\partial\left(\bullet\right)}{\partial x}+N_{yy}^0\frac{\partial\left(\bullet\right)}{\partial y}\right) \qquad \text{(3a-g)}$$

where N_{xx}^0, N_{yy}^0 and N_{xy}^0 are introduced initial stresses acting along corresponding directions.

Elements of matrixes A, B, and D are:

$$\begin{vmatrix} A_{11} & A_{12} & A_{16} \\ A_{12} & A_{22} & A_{26} \\ A_{16} & A_{26} & A_{66} \end{vmatrix}=\begin{vmatrix} A_{11}^{shell} & A_{12}^{shell} & 0 \\ A_{12}^{shell} & A_{22}^{shell} & 0 \\ 0 & 0 & A_{66}^{shell} \end{vmatrix}+\begin{vmatrix} \frac{E_sA_s}{d_s} & 0 & 0 \\ 0 & \frac{E_rA_r}{d_r} & 0 \\ 0 & 0 & 0 \end{vmatrix}$$

$$\begin{vmatrix} D_{11} & D_{12} & D_{16} \\ D_{12} & D_{22} & D_{26} \\ D_{16} & D_{26} & D_{66} \end{vmatrix}=\begin{vmatrix} D_{11}^{shell} & D_{12}^{shell} & 0 \\ D_{12}^{shell} & D_{22}^{shell} & 0 \\ 0 & 0 & D_{66}^{shell} \end{vmatrix}$$

$$+\begin{vmatrix} \frac{E_s}{d_s}\left(I_s^c+e_s^2A_s\right) & 0 & 0 \\ 0 & \frac{E_r}{d_r}\left(I_r^c+e_r^2A_r\right) & 0 \\ 0 & 0 & \frac{G_sJ_s}{d_s}+\frac{G_rJ_r}{d_r} \end{vmatrix}$$

In above equations c_1 and c_2 coefficients introduced to implement different shell theories or strain-displacement relations (see also [11]).

Accordingly, when

- $c_1=c_2=1$ the first approximation of Sander's- Koiter shell theory,
- $c_1=1, c_2=0$ Love's shell theory,
- $c_1=c_2=0$ Donnell's Shell theory.

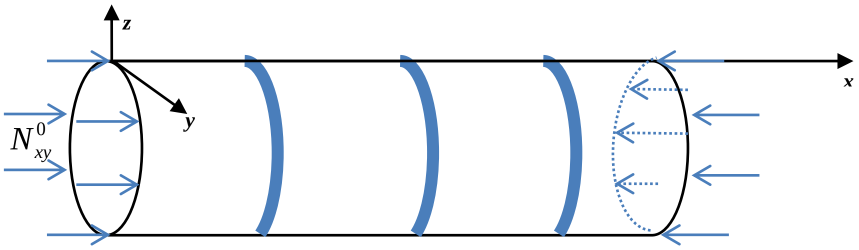

Figure 1: Orthotropic stiffened cylindrical shell under axial compressive loads.

Geometrical representation is given in Figure 1.

Let's $N^{(0)}_{xx} = -L_1\tilde{p}, \quad N^{(0)}_{yy} = -L_2\tilde{p}$, and $N^{(0)}_{xy} = 0$, where L_1 and L_2 are some constants. Next, we will assume $A_{16} = A_{26} = 0$ and cylindrical shell is closed with simply supported boundary conditions on both edges: $x = 0$ and $x = L$.

Next the solutions of Equations (1) we will search in the following form

$$U_1 = \bar{u}_1 \cos\left(\frac{\pi m x}{L}\right)\cos\left(\frac{ny}{R}\right), \qquad U_2 = \bar{u}_2 \sin\left(\frac{\pi m x}{L}\right)\sin\left(\frac{ny}{R}\right)$$

$$U_3 = \bar{u}_3 \sin\left(\frac{\pi m x}{L}\right)\cos\left(\frac{ny}{R}\right)$$

with unknown coefficients $\bar{u}_i\left(i = 1,2,3\right)$. It is obvious that mentioned solutions satisfying simply supported boundary conditions. Inserting solutions $U_i\left(x,y\right)\left(i = 1,2,3\right)$ in to Eq (1) and averaging

$$\int_0^{2\pi}\int_0^{2\pi}\left(\bullet\right)dxdy$$

the following algebraic equation can be obtained from (1) for the unknown coefficients $\bar{u}_i\left(i = 1,2,3\right)$

$$k_{ij}\bar{u}_j = \tilde{p}g_{ij}\bar{u}_j, \left(i = 1,2,3\right) \tag{4}$$

where

$$k_{11} = A_{11}\left(\frac{\pi m}{L}\right)^2 + \left(A_{66} - B_{66}\frac{c_2}{R} + D_{66}\frac{c_2}{4R^2}\right)\left(\frac{n}{R}\right)^2 \tag{5a}$$

$$k_{13} = -\left(\frac{\pi m}{L}\right)^2 \left[\frac{A_{12}}{R} + B_{11}\left(\frac{\pi m}{L}\right)^2 + \left[B_{12} + 2B_{66} - \frac{c_2}{R} D_{66}\right]\right]\left(\frac{n}{R}\right)^2 \tag{5b}$$

$$k_{22} = \left(A_{66} + \frac{3c_2}{R} B_{66} + \frac{9c_2}{4R^2} D_{66}\right)\left(\frac{\pi m}{L}\right)^2 + \left(A_{22} + 2B_{22}\frac{c_2}{R} + D_{22}\frac{c_2}{R^2}\right)\left(\frac{n}{R}\right)^2 \tag{5c}$$

$$k_{23} = \frac{n}{R}\left\{\frac{1}{R}\left(A_{22} + B_{22}\frac{c_2}{R}\right) + \left[B_{12} + 2B_{66} + \right.\right.$$

$$\left.\left. + \frac{c_2}{R}\left(D_{12} + 3D_{66}\right)\right]\left(\frac{\pi m}{L}\right)^2 + \left(B_{22} + \frac{c_2}{R} D_{22}\right)\left(\frac{n}{R}\right)^2\right\} \tag{5d}$$

$$k_{33} = D_{11}\left(\frac{\pi m}{L}\right)^4 + D_{22}\left(\frac{n}{R}\right)^4 + 2\left(D_{12} + 2D_{66}\right)\left(\frac{\pi m}{L}\right)^2\left(\frac{n}{R}\right)^2 +$$

$$2\frac{B_{12}}{R}\left(\frac{\pi m}{L}\right)^2 + 2\frac{B_{22}}{R}\left(\frac{n}{R}\right)^2 + \frac{A_{22}}{R^2} \tag{5e}$$

$$k_{23} = k_{32}, \quad k_{13} = k_{31}, \quad k_{12} = k_{21} \tag{5f}$$

$$g_{11} = \frac{c_1 c_2}{4}\left(L_1 + L_2\right)\left(\frac{n}{R}\right)^2, \quad g_{12} = \frac{c_1 c_2}{4}\left(L_1 + L_2\right)\left(\frac{n}{R}\right)\left(\frac{\pi m}{L}\right)$$

$$g_{22} = \frac{c_2 L_2}{R} + \frac{c_1 c_2}{4}\left(L_1 + L_2\right)\left(\frac{\pi m}{L}\right)^2, \quad g_{23} = \frac{c_2 L_2}{R}\left(\frac{n}{R}\right),$$

$$g_{33} = L_1\left(\frac{\pi m}{L}\right)^2 + L_2\left(\frac{n}{R}\right)^2,$$

$$g_{23} = g_{32}, \; g_{13} = g_{31}, \quad g_{12} = g_{21} = 0 \tag{6a-g}$$

Critical load $\tilde{p}$ then can be determined from algebraic equations (4) assuming existence of nontrivial solutions

$$C_3 \tilde{p}^3 + C_2 \tilde{p}^2 - C_1 \tilde{p} + C_0 = 0 \tag{7}$$

where

$$C_0 = k_{33}\left(k_{11}k_{22} - k_{12}k_{12}\right) + k_{23}\left(k_{12}k_{23} - k_{22}k_{13}\right) + k_{13}\left(k_{12}k_{23} - k_{22}k_{13}\right)$$

$$C_1 = g_{11}\left(k_{33}k_{22} - k_{23}k_{23}\right) + g_{22}\left(k_{11}k_{33} - k_{13}k_{13}\right)$$

$$+ g_{33}\left(k_{11}k_{22} - k_{12}k_{12}\right) + 2g_{12}\left(k_{13}k_{23} - k_{12}k_{33}\right) + 2g_{23}\left(k_{12}k_{13} - k_{11}k_{23}\right)$$

$$C_2 = k_{11}\left(g_{33}g_{22} - g_{23}g_{23}\right) + k_{22}\left(g_{11}g_{33}\right)$$
$$+k_{33}\left(g_{11}g_{22} - g_{12}g_{12}\right) + 2g_{12}\left(k_{13}g_{23} - k_{12}g_{33}\right) - 2g_{11}\left(g_{23}k_{23}\right)$$
$$C_3 = g_{11}g_{23}g_{23} - g_{33}\left(g_{11}g_{22} - g_{12}g_{12}\right) \tag{8a-d}$$

Notice that the value's of c_1 and c_2 are only 0 or 1, respectively. In general (when $c_1 = 1, c_2 = 1$) the critical value for buckling load $\tilde{p}$ is determined from 3[th] order algebraic equation (7). There are some particular cases when buckling load $\tilde{p}$ is obtained from second order (when $C_3 = 0$) algebraic equation. In this case buckling load $\tilde{p} = \min\{\tilde{p}_1, \tilde{p}_2\}$ (if $\tilde{p}_1 > 0, \tilde{p}_2 > 0$), and $\tilde{p} = \tilde{p}_1$ (if $\tilde{p}_1 > 0, \tilde{p}_2 < 0$),

where $\tilde{p}_{1,2} = \left(C_1 \pm \sqrt{C_1^2 - 4C_0C_2}\right) / 2C_2$.

When $C_3 = C_2 = 0$, buckling load $\tilde{p}$ is determined as $\tilde{p} = C_0 / C_1$. Expression for C_3 can be simplified

$$C_3 = -4c_1c_2L_2\left(L_1 + L_2\right)\left[-4\left(c_2 - 1\right)L_2 + \pi^2 L_1\right] \tag{9}$$

From (9) it can be seen that $C_3 = 0$ in the following cases:

1) $c_1 = 0, c_2 = 0$ (Donnell's theory; in this case from (8c-d) it follows that not only $C_3 = 0$ but also $C_2 = 0$ and algebraic equation (7) is first order);

2) $c_1 = 0, c_2 = 1$;

3) $c_1 = 1, c_2 = 0$ (Love's theory);

4) $L_2 = 0$ (Axial compression);

5) $L_1 = -L_2$;

6) $L_1 = 0$.

PARTICULAR CASES

R. Jones Results

From formulae (7) Jones [12] results can be derived: stability criterion for stiffened orthotropic circular cylindrical shells. For that reason, we need to assume that $c_1 = c_2 = 0$, then $C_2 = C_3 = 0$. From (7) $\tilde{p}$ can be obtained in the following way

$$\tilde{p} = \frac{C_0}{C_1} = \frac{1}{g_{33}}\left[k_{33} + k_{23}\frac{k_{13}k_{12} - k_{11}k_{23}}{k_{11}k_{22} - k_{12}k_{12}} + k_{13}\frac{k_{12}k_{23} - k_{13}k_{22}}{k_{11}k_{22} - k_{12}k_{12}}\right]$$

Results From Leissa [16]; Mikulas & McElman [20]

From formulae (7) Leissa [16] and Mikulas & McElman [20] results can be derived. Assuming a cylindrical shell is isotropic with Young's modulus E and Poisson's ratio ν, from (7) $\tilde{p}$ can be obtained in the following way

$$\tilde{p} = \tilde{p}\left(\frac{m^2L^2}{D\pi^2}\right)\left(\delta^2 L_2 + L_1\right) = m^4(1+\delta^2)^2$$

$$+m^4\left[\frac{E_sI_s}{Dd_s} + \delta^2\left(\frac{G_sJ_s}{Dd_s} + \frac{G_rJ_r}{Dd_r}\right) + \delta^4\frac{E_rI_r}{Dd_r}\right]$$

$$+\frac{12L^4\left(1-\nu^2\right)}{h^2R^2}\left[\frac{1+\bar{S}\Lambda_s + \bar{R}\Lambda_r + \bar{S}\,\bar{R}\Lambda_{rs}}{\Lambda}\right] \quad (10)$$

where,

$$\Lambda_s = 1 + 2\lambda^2\left(e_s/R\right)\left(\delta^2 - \nu\right) + \lambda^4(e_s/R)^2(1+\delta^2)^2$$

$$\Lambda_r = 1 + 2n^2\left(e_r/R\right)\left(1-\delta^2\nu\right) + n^4(e_r/R)^2(1+\delta^2)^2$$

$$\Lambda_{rs} = \lambda^2 n^2\left[\delta^2\left(1-\nu^2\right) + 2\left(1+\nu\right)(e_s/R)^2\right] +$$

$$+n^4\left[1-\nu^2 + 2\delta^2\left(1+\nu\right)(e_r/R)^2\right] + 2n^2\left(1-\nu^2\right)(e_s/R)^2 +$$

$$+2n^2\left(1-\nu^2\right)(e_r/R)^2 + 2n^4(1+\nu)^2\left(e_s/R\right)\left(e_r/R\right) + 1 - \nu^2\Lambda =$$

$$= (1+\delta^2)^2 + 2\delta^2\left(1+\nu\right)\left(\bar{R}+\bar{S}\right) + \left(1-\nu^2\right)\left[\bar{S} + \delta^4\bar{R} + 2\delta^2\bar{S}\,\bar{R}\left(1+\nu\right)\right]$$

$$\lambda = \frac{\pi mR}{L}, \quad \bar{S} = \frac{E_sA_s}{Ehd_s}, \quad \bar{R} = \frac{E_rA_r}{Ehd_r}$$

$$\delta = \frac{n}{\lambda} = \frac{nL}{\pi mR}, \quad D = \frac{Eh^3}{12\left(1-\nu^2\right)}$$

Formulae (10) is consistent to Leissa's [16] notations.

NUMERICAL RESULTS AND DISCUSSION

Ring-Stiffened Circular Cylindrical Shell With Two Isotropic Layers Under Axial Compression

A specific numerical example is given to illustrate application of the theory. The results are compared to similar problems previously studied (see Jones [12]).

For example, the stability of a ring-stiffened circular cylindrical shell with two isotropic layers under axial compression is considered. The properties of the layers are

$E_1 = 44 \times 10^6\, psi,\ \nu_1 = 0,\ t_1 = 0.04in$ and

$E_2 = 2 \times 10^6\, psi, \nu_2 = 0.4, t_2 = 0.3in$

where t_1 and t_2 are the thickness of first and second layers. The rings are of rectangular cross section with a height of $0.25in$ and a thickness of $0.06in$. The rings are on the inner surface of layer one, and have the same material properties as layer one. The shell has a length of $L = 12in$ and a radius of $R = 6in$ to the middle surface of layer one (which, in this case, is also the reference surface).

For comparison purposes the behavior of non-dimensional axial load $N_{xx}^0 / E_1 h$, ($h = t_1 + t_2$ is a total thickness of the shell) with respect of dimensionless ring spacing is shown in Figure 2 using Donnell's, Sanders and Love's theories (Red line illustrates Donnell's, blue line-Sander's, and gray line-Love's theories, respectively.

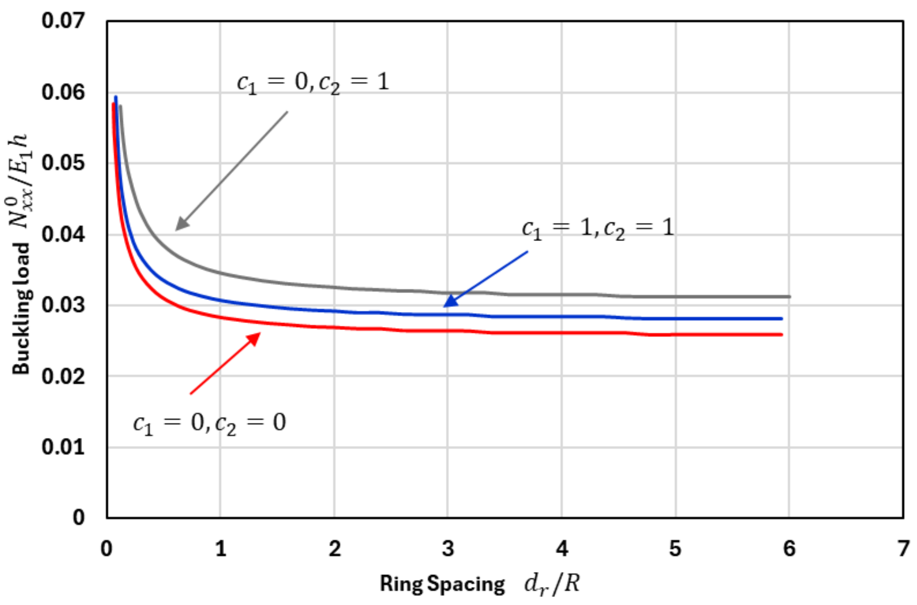

Figure 2: Buckling load of a ring-stiffened, two-layered circular cylindrical shell versus ring spacing. Red line-Donnell's theory; Blue line-Sander's theory; Gray line-Love's theory.

Each of these theories show a limiting level of bucking load with increasing ring spacing. The Sunder's theory lies between Donnell's and Love's theories. In some cases, the difference between presented theories can approach as much as 5~30% (More investigation is needed for buckling load, versus modulus of elasticity of the ring, and ring spacing). Notice that red line is consistent to Jones [12] result calculated with a formula (25) in the mentioned work.

Isotropic Ring-Stiffened Circular Cylindrical Shell Under Axial Compression

The material properties of the shell are

$E_1 = 44 \times 10^6\, psi\ \ \nu_1 = 0\ \ h = t_1 = 0.34in$

The rings are on the inner surface of the shell. The shell has a length of $L = 12in$ and a radius of $R = 6in$ to the middle surface of shell (which, in this case, is also the reference surface). Notice that red line is consistent to McElman's [19] result, calculated with a formula (33) in the mentioned work.

From Figure 3 it can be seen that for large values of ring spacing using Donnell's theory (red line, $c_1 = c_2 = 0$) and Love's theory (gray line, $c_1 = 0, c_2 = 1$), it provides a close value for critical buckling load. In some cases the difference between Donnell's, Sander's and Love's theories is ~15%. which should be taken into account for determination of bucking load .

Based on Equations (3)–(8) some particular cases are considered the next.

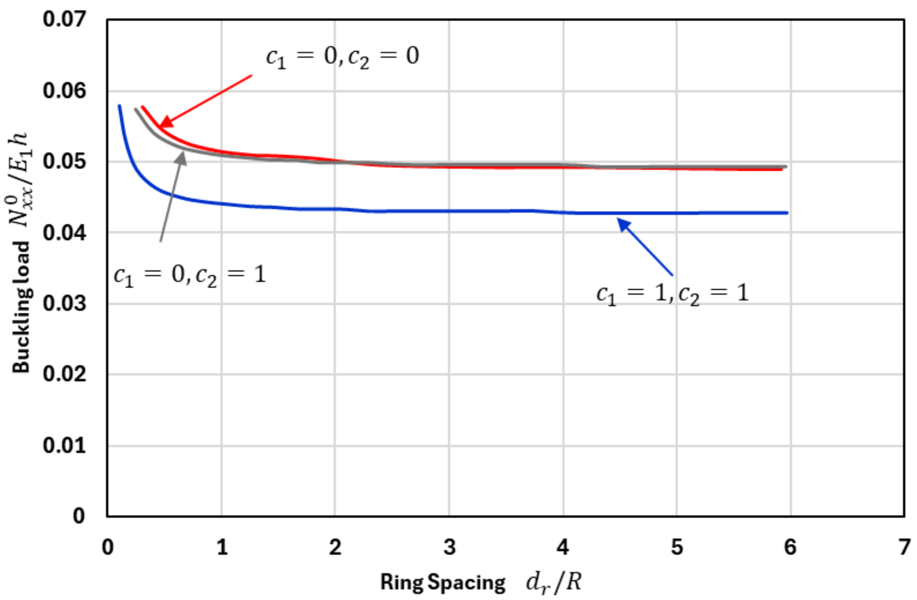

Figure 3: Buckling load of a ring-stiffened, isotropic circular cylindrical shell versus ring spacing. Red line-Donnell's theory; Blue line-Sander's theory; Gray line-Love's theory.

Cross -Ply with N odd (symmetric) Laminated Layers

A cross-ply laminate has N unidirectional reinforced layers with principal material directions oriented in an alternating manner at 0° and 90° to the laminate coordinate axes. The fiber direction of odd-numbered layers is the x direction of the laminate. The fiber direction of even-numbered layers is then the y direction of the laminate. Two geometrical parameters are important: N, the total number of layers, and M, the ratio of the total thickness of odd-numbered layers to the total thickness of even-numbered layers (called the cross-ply ratio). Thus,

$$M = \sum_{k=odd} h_k \Big/ \sum_{k=even} h_k ,$$

and the ratio of principal lamina stiffness
$F = E_2 / E_1$.

Following notations are given bellow:

$$\tilde{A}_{11} = \frac{M+F}{1+M} + \mu_s , \tilde{A}_{22} = \frac{1+MF}{1+M} + \mu_r , \tilde{A}_{12} = \nu_{12} F , \; \tilde{A}_{ij} = A_{ij}\left(1-\nu_{12}\nu_{21}\right) / E_1 h$$

$$\tilde{B}_{11} = \frac{M\left(F-1\right)}{N(1+M)^2} h + \mu_s e_s , \quad \tilde{B}_{22} = -\frac{M\left(F-1\right)}{N(1+M)^2} h + \mu_r e_r ,$$

$$\tilde{B}_{ij} = B_{ij}\left(1-\nu_{12}\nu_{21}\right) / E_1 h,$$

$$\tilde{D}_{11} = \frac{h^2}{12}\left[R\left(F-1\right)+1\right] + \mu_s e_s^2 + \mu_s I_1 L^2,$$

$$\tilde{D}_{22} = \frac{h^2}{12}\left[R\left(F-1\right)+1\right] + \mu_r e_r^2 + \mu_r I_2 L^2,$$

$$\tilde{D}_{12} = \frac{h^2}{12}\nu_{12} F , \quad \tilde{D}_{66} = \frac{h^2}{12} G + \left(\eta_r + \eta_s\right) L^2$$

$$\tilde{D}_{12} = \frac{h^2}{12}\nu_{12} F , \quad \tilde{D}_{66} = \frac{h^2}{12} G + \left(\eta_r + \eta_s\right) L^2$$

$$\tilde{D}_{ij} = D_{ij}\left(1-\nu_{12}\nu_{21}\right) / E_1 h$$

The expressions for k_{ij} can be simplified as

$$k_{ij} = \frac{L^2\left(1-\nu_{12}\nu_{21}\right)}{E_1 h}\tilde{k}_{ij}$$

$$\tilde{k}_{11} = (\pi m)^2\left(\frac{M+F}{M+1} + \mu_s\right) + n^2\left(\frac{L}{R}\right)^2 G + c_2\frac{1}{4}\left(\frac{L}{R}\right)^2\left[\frac{1}{12}\left(\frac{h}{R}\right)^2 G + \left(\frac{L}{R}\right)^2\left(\eta_s + \eta_r\right)\right]$$

$$\tilde{k}_{12} = -\left(\pi mn\right)\frac{L}{R}\{\nu_{12} F + G - c_2\frac{3}{4}[\frac{1}{12}\left(\frac{h}{R}\right)^2 G + \left(\frac{L}{R}\right)^2\left(\eta_s + \eta_r\right)]$$

$$\tilde{k}_{13} = -(\pi m)\left\{\nu_{12}F\frac{L}{R} + (\pi m)\left[\frac{M(F-1)}{N(1+M)^2}\frac{h}{L} + \mu_s\frac{e_s}{L}\right]\right.$$

$$\left. -c_2 n^2\left(\frac{L}{R}\right)^2\left[\frac{1}{12}\left(\frac{h}{R}\right)\left(\frac{h}{L}\right)G + \left(\frac{L}{R}\right)(\eta_s+\eta_r)\right]\right\}$$

$$\tilde{k}_{22} = (\pi m)^2\left\{G + c_2\frac{9}{4}\left(\frac{L}{R}\right)^2\left[\frac{1}{12}\left(\frac{h}{R}\right)^2 G + \left(\frac{L}{R}\right)^2(\eta_s+\eta_r)\right]\right\}$$

$$+n^2\left(\frac{L}{R}\right)^2\left\{-\frac{MF+1}{M+1} + \mu_r - 2c_2\left[-\frac{M(F-1)}{N(M+1)^2}\frac{h}{R} + \mu_r\frac{e_r}{R}\right]\right.$$

$$\left. +c_2\left[\frac{1}{12}\left(\frac{h}{R}\right)^2(F+R-FR) + \mu_r\left(\frac{e_r}{R}\right)^2 + \mu_r I_2\left(\frac{h}{R}\right)^2\right]\right\}$$

$$\tilde{k}_{23} = n\left(\frac{L}{R}\right)^2\left\{\frac{MF+1}{M+1} + \mu_r + c_2\left[-\frac{M(F-1)}{N(M+1)^2}\frac{h}{R} + \mu_r\frac{e_r}{R}\right] + \right.$$

$$\left.(\pi m)^2 n c_2\left[\frac{1}{12}\left(\frac{h}{R}\right)^2\nu_{12}F + 3\frac{1}{12}\left(\frac{h}{R}\right)^2 G + 3(\eta_s+\eta_r)\left(\frac{L}{R}\right)^2\right]\right\} +$$

$$+n^3\left(\frac{L}{R}\right)^2\left\{-\frac{M(F-1)}{N(M+1)^2}\frac{h}{R} + \mu_r\frac{e_r}{R} + \right.$$

$$\left. +c_2\left[\frac{1}{12}\left(\frac{h}{R}\right)^2(F+R-FR) + \mu_r\left(\frac{e_r}{R}\right)^2 + \mu_r I_2\left(\frac{h}{R}\right)^2\right]\right\}$$

$$\tilde{k}_{33} = (\pi m)^4\left\{\frac{1}{12}\left(\frac{h}{L}\right)^2(FR-R+1) + \mu_s\left(\frac{e_s}{R}\right)^2 + \mu_s I_1\right\} +$$

$$2(\pi m)^2 n^2\frac{1}{12}\left(\frac{h}{R}\right)^2\nu_{12}F + 4(\pi m)^2 n^2\left\{\frac{1}{12}\left(\frac{h}{R}\right)^2 G + (\eta_s+\eta_r)\left(\frac{L}{R}\right)^2\right\}$$

$$+n^4\left(\frac{L}{R}\right)^2\left\{\frac{1}{12}\left(\frac{h}{R}\right)^2(F+R-FR) + \mu_r\left(\frac{e_r}{R}\right)^2 + \mu_r I_2\left(\frac{h}{R}\right)^2\right.$$

$$\left. +2n^2\left(\frac{L}{R}\right)^2\left[-\frac{M(F-1)}{N(F+1)^2}\frac{h}{R} + \mu_r\frac{e_r}{R}\right] + \left(\frac{L}{R}\right)^2\left[\frac{MF+1}{1+M} + \mu_r\right]\right\}$$

Numerical example is given to illustrate application of the theory for cross-ply laminated shells. For this example, the stability of a ring-stiffened circular cylindrical shell with two layers under axial compression is considered (we assume that $F = 2, M = 1, \nu_{12} = 0.25$). Parameters of stiffeners and rings are: $\mu_s = \eta_r = \eta_s = 0$, $e_r = 0.01, e_s = 0$. The rings are of rectangular cross section with a height of $0.25 in$ and a thickness of $0.06\ in$. The shell has a length of $L = 12 in$ and a radius of $R = 6 in$ to the middle surface of layer one (which, in this case, is also the reference surface).

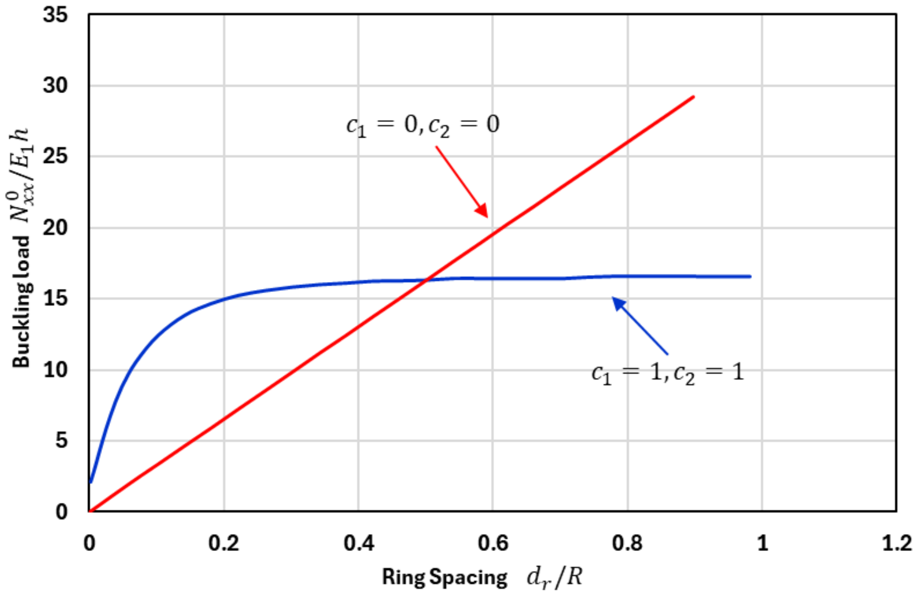

Figure 4: Buckling load of a ring-stiffened, cross-ply circular cylindrical shell versus ring rigidity. Red line-Donnell's theory; Blue line-Sander's theory**.**

Figure 4 provides the value of buckling load of a ring-stiffened, cross-ply circular cylindrical shell versus ring rigidity. Red line represents Donnell's theory, blue line-Sander's theory, and gray line-Love's theory for small values of rigidity of rings. From this numerical calculation it can be seen that buckling load is essentially different for different theories: Donnell's, Sander's and Love's, respectively. It is visible that Love's theory cannot provide values for critical buckling load for large values of rigidity of the rings.

SOME APPLICATIONS IN INDUSTRY

Composite vessel designs with unique features and attachments generally require reinforcement to increase the load carrying capacity for nozzle stresses and torsional loads; orthogonal stiffeners, thicker cross sections, and reinforcement layers are common to increase the load capacity. Analytical tools that allow each layer to have different elastic and material properties will be required to allow the composite designer to optimize using functionally graded material sets. Analysis approaches like those demonstrated will allow future designers to match material properties to the design need. These techniques can also be used to analyze repairs and alterations to FRP (fiber reinforced plastic) vessels.

Stiffened cylindrical shells (vessels) have broad applications. For example, Space Shuttle external tank (stiffened cylindrical vessel) was designed for liquid hydrogen fuel and liquid oxygen oxidizer. Other applications of stiffened cylindrical vessels are in nuclear industry, for storing different types of nuclear and chemical components.

More complex designs and configurations with integral nozzles and stiffened cylindrical vessels require more sophisticated analysis tools and a design-by-stress type of analysis.

Note that stiffened cylindrical shells have tendency of local deformations (global and local buckling). Existing classical theories do not allow them to capture all mentioned deformations (especially the local deformations). Modified Sander's theory is a tool that can be used to design more complex vessels and get more accurate behavior of shells (stresses, strains, displacements) locally and globally.

CONCLUSION

The current study presents theoretical formulations of stability analysis for stiffened cylindrical shells. Theory is developed based on Sanders-Koiter assumptions. An example of buckling of stiffened cylindrical shell under axial compression loads demonstrated disagreements between various theories (Donnel, Love-Kirckhoff) compared with Sanders-Koiter assumptions. Buckling critical loads derived and demonstrated Buckling load variation versus rings spacing. Numerical examples are given to illustrate application of the proposed theory and analytically derived formulas comprised of buckling loads.

The results will be practical to investigate the behavior of the composite structures under different types of external factors (i.e. mechanical forces, thermal loads, earthquake etc). Thus, the results will predict a design life more accurately for composite vessels which is significantly greater than similar vessels constructed using current industry standards.

REFERENCES

1. Baruch, M., Singer, J., Effect of eccentricity of stiffeners on the general instability of stiffened cylindrical shells under hydrostatic pressure, Journal of Mechanical Engineering Science, 5, 1, pp. 23-27, 1963.
2. Batdorf, S.B. et al, Critical combinations of shear and longitudinal direct stress for long plates with transverse curvature. TN 1347, NACA, 1947.
3. Becker, H., Handbook of structural stability. Part VI-strength of stiffened curved plates and shells, TN 3786, NACA, 1958.
4. Birman, V., Extension of Vlasov's Semi-membrane Theory to Reinforced Composite Shells, Transactions of the ASME, 462/Vol. 59, JUNE 1992.
5. Birman, V., Thermal Dynamic Problems of Reinforced Composite Cylinders, Journal of Applied Mechanics DECEMBER, Vol. 57 / 941, 1990.
6. Card, M.F., Jones, R.M., Experimental and theoretical results for buckling of eccentrically stiffened cylinders, TN-D-3639, NASA, 1966.
7. Chandrashekara, K. Pavan Kumar, D. V.T.G., Assessment of shell theories for the static analysis of cross-ply laminated circular cylindrical shells, Thin Walled Structures 22, 291-318, 1995.
8. Donnell, L.H., A new theory for the buckling of thin cylinders under axial compression and bending. Trans ASME, 56:795–806, 1934.

9. Gerard, G., Becker, H., Handbook of structural stability. Part III-Buckling of curved plates and shells, TN 3783, NACA, 1957.
10. James, P.P., and Ralph, 0.W., Local buckling of longitudinally stiffened curved plates, NASA TECHNICAL NOTE D-750, 1961.
11. Jaunky, N., and Knight, Norman, F., Jr., An assessment of shell theories for buckling of circular cylindrical laminated composite panels loaded in axial compression. Int. J. Solids and Structures, 36 , 3799-3820, 1999.
12. Jones, R.M., Buckling of circular cylindrical shells with multiple orthotropic layers and eccentric stiffeners, AIAA Journal, v.6, 12, 1968, pp. 2301-2305.
13. Jones, R. M., Mechanics of Composite Materials, McGraw-Hill (1975).
14. Knight, N.F., Starnes J.H., Developments in cylindrical shell stability analysis, Proceedings of the 38th AIAA/ASME/ASC/AHS/ASCE Structures, Structural Dynamics, and Materials Conference, Kissimmee, Florida, April 1997, pp 1933-1947. Also AIAA Paper No AIAA-97-1076, 1997.
15. Koiter, W.T., A consistent first approximation in general theory of thin elastic shells. The theory of thin elastic shells, Proceedings IUTAM Symposium, Delft, North Holland, Amsterdam, The Netherlands, pp 12-33, 1959.
16. Leissa, A. W., Vibration of Shells. NASA SP-288 (1973).
17. Love, A.E.H., On the small free vibrations and deformations of the elastic shells, Phil. Trans. R. Sot Lond. A 17, 401-546, 1988.
18. McElman, J.A., Mikulas, M.M., Stein, M., Static and dynamic effects of eccentric stiffening of plates and cylindrical shells, AIAA Journal, 4, 5, pp.887-894, 1966.
19. McElman, J.A., Eccentrically stiffened Shallow shells of double curvature., NASA-TN-D-3826, February 1967.
20. Mikulas, M.M., McElman, J.A., On free vibrations of eccentrically stiffened cylindrical shells and flat plates, NASA-TN-D-3010, Sept., 1965.
21. Nemeth M.P. Nondimensional parameters and equations for buckling of anisotropic shallow shells, ASME Journal of Applied Mechanics, 61, 664-669, 1994.
22. Nemeth M.P., A Leonard-Sanders-Budiansky-Koiter-Type Nonlinear Shell Theory with a Hierarchy of Transverse-Shearing Deformations, NASA/TP–2013-218025, July, 2013.
23. Noor A.K., Bibliography of monographs and surveys on shells, Applied Mechanics Review 43 (9), 1990.
24. Peterson, J.P., and Whitley, R.O., Local Buckling of Longitudinally Stiffened Curved Plates, NASA, TN D-750, 1961.
25. Rafel, N., Effect of normal pressure on the critical compressive stress of curved sheet. WRL-258, NACA, 1942.
26. Rafel, N., and Sandlin, C.W. Jr., Effect of normal pressure on the critical compressive and shear stress of curved sheet. WRL-57, NACA, 1944.
27. Reddy, J.N., A Layerwise Shell Theory with Applications to Buckling and Vibration of Cross-Ply Laminated Stiffened Circular Cylindrical Shells. *CCMS-92-01*, Virginia Polytechnic Institute and State University, 1992.
28. Sanders, J.L., An improved first-approximation theory for thin shells, NASA Tech. Rep. R-24 1959.
29. Sanders, J.L., Non-linear theories for thin shells, Quart J Appl. Math, 21:21–36, 1963.
30. Schildcrout, M., Stein, M., Critical combination of shear and direct axial stress for curved rectangular panels, TN 1928, NACA, 1949.

31. Simitses, G.J., General instability of eccentrically stiffened cylindrical panels, J. AIRCRAFT VOL. 8, NO. 7, pp. 569-575,1971.
32. Stein, M., and Fralich, R.W., Critical shear stress of infinitely long, simply supported plate with transverse stiffeners technical note No. 1851., 1949.
33. Teng, G. J., Buckling of thin shells]: recent advances and trends. Applied Mechanics Review 49 (4), 263-274, 1996.
34. Viswanathan, A.V., and Tamakun M., Elastic Stability of Biaxially Loaded Longitudinally Stiffened Composite Structures, AIAA Journal, Vol. 11, No. 11, November, 1973.
35. Yi-Wei, L., Elishakoff, I., Starnes Jr., J. H., Bushnell, D. Effect of the thickness variation and initial imperfection on buckling of composite cylindrical shells] asymptotic analysis and numerical results by BOSOR3 and PANDA2, International Journal of Solids and Structures 34, 3755-3767, 1997.

APPENDIX

KINEMATIC RELATIONS FROM SANDERS FORMULATION

The tangential and normal displacement fields of a material point (x, y, ζ) of a cylindrical shell are expressed in orthogonal principal-curvature coordinates as

$$u_1(x,y,z) = U_1(x,y) + \zeta(\varphi_1 - \varphi_n \varphi_2)$$

$$u_2(x,y,z) = U_2(x,y) + \zeta(\varphi_2 + \varphi_n \varphi_1$$

$$u_3(x,y,z) = U_3(x,y) - \frac{1}{2}\zeta(\varphi_1^2 + \varphi_2^2)$$

Where x is an axial coordinate, y is a circumferential arc length coordinate, ζ is an outward radial coordinate with its origin at the middle-surface; The middle surface has radius R and length L; $U_i(x,y)$, $(i = 1,2,3)$ are middle-surface displacements ($U_1(x,y)$ is an axial displacement, $U_2(x,y)$ is a circumferential displacement and $U_3(x,y)$ is a radial displacement).

The linear rotation vectors components that correspond to the rotations of differential elements coincides to the middle-surface normal at the point (x, y) and expressed as

$$\varphi_1 = -\frac{\partial U_3}{\partial x};$$

$$\varphi_2 = c_2 \frac{U_2}{R} - \frac{\partial U_3}{\partial y};$$

$$\varphi_n = \frac{1}{2} c_2 \left[\frac{\partial U_2}{\partial x} - \frac{\partial U_1}{\partial y} \right];$$

The nonlinear membrane strains components of the cylindrical middle-surface are given in Sanders original paper [29] and expressed as

$$\varepsilon_{11}^{(0)}=\frac{\partial U_1}{\partial x}+\frac{1}{2}\left[\varphi_1^2+c_1\varphi_n^2\right];$$

$$\varepsilon_{22}^{(0)}=\frac{\partial U_2}{\partial y}+\frac{U_3}{R}+\frac{1}{2}\left[\varphi_2^2+c_1\varphi_n^2\right]$$

$$\varepsilon_{12}^{(0)}=\frac{1}{2}\left[\frac{\partial U_2}{\partial x}+\frac{\partial U_1}{\partial y}+c_1\varphi_1\varphi_2\right]$$

Bending strains of the middle Surface of cylindrical Shell, associated with changes in surface curvature and torsion caused by deformations are given by

$$k_{11}^{(0)}=\frac{\partial\varphi_1}{\partial x}\ ;\ k_{22}^{(0)}=\frac{\partial\varphi_2}{\partial y};\ k_{12}^{(0)}=\frac{\partial\varphi_1}{\partial y}+\frac{\partial\varphi_2}{\partial x}+\frac{c_2}{R}\varphi_n$$

In equations two parameters c_1, and c_2 are introduced to trace the contributions of various terms to the equations governing nonlinear and buckling phenomena. These two parameters c_1, and c_2 are equal to unity or zero.

<u>Information about authors:</u>

M.F. Alam. Ph.D. Candidate , Department of Aerospace and Mechanical Engineering, University of Texas at El Paso, 500 W University Ave, El Paso, 79928, Texas, United States.
E-mail: malam8@miners.utep.edu

A. Banafshi. Ph.D. Candidate, Department of Aerospace and Mechanical Engineering, University of Texas at El Paso, 500 W University Ave, El Paso, 79928, Texas, United States.
E-mail: abanafshi@miners.utep.edu

C. Moriel. Ph.D. Candidate , Department of Aerospace and Mechanical Engineering, University of Texas at El Paso, 500 W University Ave, El Paso, 79928, Texas, United States.
E-mail: emoriel2@miners.utep.edu

D. J. Hasanyan. Sr Specialist, Copeland Inc., Sidney, OH, USA,
E-mail: davreshh@yahoo.com

A.D. Hasanyan. Assistant Professor, Department of Aerospace and Mechanical Engineering, University of Texas at El Paso, 500 W University Ave, El Paso, 79928, Texas, United States.
E-mail: adhasanyan@utep.edu

Received 12, March, 2026